#1358

Radar Imagery for Precision Crop and Soil Management

M. Susan Moran, Daniel C. Hymer, and Jiaguo Qi
USDA-ARS U.S. Water Conservation Laboratory
Phoenix, Arizona

Yann Kerr
Centre d'Etudes Spatiales de la Biosphere
Toulouse, France

ABSTRACT

Studies during the past 25 yrs have shown that measurements of surface reflectance and temperature (termed optical remote sensing) are useful for monitoring crop and soil conditions. Far less attention has been given to the use of radar imagery, even though Synthetic Aperture Radar (SAR) systems have the advantages of cloud penetration, all-weather coverage, high spatial resolution, day–night acquisitions, and signal independence of the solar illumination angle. In this study, we obtained coincident optical and SAR images of an agricultural area to investigate the use of SAR imagery for precision farm management. Results showed that SAR imagery was sensitive to variations in field tillage, surface soil moisture and vegetation density. The coincident optical images proved useful in interpretation of the response of SAR backscatter to soil and plant conditions.

INTRODUCTION

By the year 2000, there will be about 10 earth-observation satellites supporting optical sensors with the spatial, spectral and temporal resolutions suitable for many farm management applications (Moran et al., 1997a). These optical sensors provide information in the reflective and thermal emissive portions of the electromagnetic spectrum. In a multitude of studies, this information has been used for such important farm applications as scheduling irrigations, predicting crop yields, and detecting certain plant diseases and insect infestations (see review by Hatfield & Pinter, 1993). Although optical remote sensing is a powerful farm management tool, there are some serious limitations that have restricted farm management applications. For example, acquisitions are limited to cloudfree sky conditions; the signal is attenuated by the atmosphere; and image interpretation is a complex function of the sun/sensor/target geometry. An alternative to the use of optical remote sensing for farm management is the use of radar backscattering data obtained from Synthetic Aperture Radar (SAR) sensors. There are currently four SAR sensors aboard polar-orbiting satellites, and there are plans for two more by the year 2000.

 Proceedings of the Fourth International Conference on Precision Agriculture.

SAR sensors measure the spatial distribution of surface reflectivity in the microwave spectrum. The radar transmits a pulse and then measures the time delay and strength of the reflected echo (i.e., amplitude and phase measurements), where the amplitude is called the radar backscatter (σ^o). The scattering behavior of the SAR signal is governed by the dielectric properties of both soil and vegetation, and the geometric configuration of the scattering elements (soil roughness, leaves, stalks and fruit) with respect to the wavelength, direction and polarization of the incident wave. SAR systems have the advantages of cloud penetration, all-weather coverage, high spatial resolution, day–night acquisitions, and signal independence of the solar illumination angle (Table 1). These advantages allow SAR images to meet the rigid data requirements involved with precision farm management (PFM) decisions. Furthermore, for PFM applications, several inherent disadvantages of SAR imagery (Table 1) are countered by the *a priori* information generally available from farm managers, such as cultivation practices, crop type, planting date, row direction, soil type, and topography (particularly with laser-leveled or terraced fields).

The greatest weakness of SAR data for precision farming is the poor understanding of the response of SAR σ^o to agricultural soil and plant conditions. Research in the optical region has benefitted from three fortuitous circumstances: (i) the LACIE and AgRISTARS Programs, (ii) availability of inexpensive, handheld optical sensors, and (iii) access to reliable optical images from orbiting sensors, particularly Landsat TM and SPOT HRV. The Large Area Crop Inventory Experiment (LACIE) and AgRISTARS Programs defined the physics of relations between optical measurements and biophysical properties of crop canopies and soils. These pioneering programs established the potential of optical remote sensing for crop management, and inspired many subsequent studies of agricultural remote sensing. Subsequent studies advanced the science based on easy and often-inexpensive access to optical data obtained with handheld, airborne or satellite-based sensors. SAR research has not had such advantages. First, there has not been a research effort of the magnitude of the LACIE and AgRISTARS Programs. Second, there are no commercially-available, inexpensive, ground- or aircraft-based SAR sensors for intensive field experiments. Third, up until this decade, there have been no SAR sensors aboard polar-orbiting satellites (Table 2). These limitations make field studies of SAR applications for agricultural management very difficult at best.

In the study presented here, we attempted to capitalize on the good understanding of the response of the optical data to plant–soil conditions in order to interpret SAR images of an agricultural region. For five dates in 1995 through 1997, we acquired pairs of images from the Landsat TM sensor and the ERS-2 SAR sensor covering the University of Arizona Maricopa Agricultural Center in central Arizona. The information obtained from multispectral reflectance (ρ) and temperature (T_s) measurements made with the TM sensor was used to interpret the signal received by the ERS-2 C-band SAR sensor. In particular, we focused on the determination of within-field variations in

- soil roughness (related to tillage, subsidence or erosion);
- vegetation density (related to seeding, crop vigor and pest infestations); and
- surface soil moisture condition (related to monitoring irrigation efficacy, soil texture).

Table 1. Complementarity of optical and SAR remote sensing. The pros and cons of these data as a source of crop and soil information for precision agriculture applications.

Issue	Optical	SAR
Atmospheric attenuation	CON: Limited to periods of cloudfree sky conditions	PRO: Characterized by cloud penetration and all-weather coverage
	CON: Sensitive to atmospheric scattering and absorption	PRO: Independent of atmospheric scattering and absorption
		CON: Characterized by speckle †
Sun–Sensor –Target Geometry	CON: Surface temperature (T_s) and reflectance (ρ) are a complex function of solar and viewing angles (θ_z and θ_v, respectively)	PRO: SAR provides its own energy source; it is independent of θ_z and maintains a relatively constant θ_v
	CON: Reflectance measurements are limited to daylight hours	PRO: SAR allows acquisition 24h day^{-1}
	CON: Measurements of surface T_s and ρ are a complex function of topography	CON: SAR backscatter is a function of topography, though the correction with available DEM data is relatively straight-forward
Sensitivity to soil and vegetation conditions	PRO: Nominally independent of small-scale soil roughness conditions	CON: Very sensitive to soil roughness conditions, particularly at roughness scales similar to the wavelength (2–6 cm)
	CON: The signal from soil is attenuated by the signal from overlying vegetation	CON: The signal from soil is attenuated by the signal from overlying vegetation
	PRO: A good theoretical and empirical basis for application in farm management	CON: Poor understanding of the response of SAR backscatter to agricultural soil/plant conditions
Data availability	PRO: Orbiting sensors characterized by high spatial resolution (10–120 m) and wide coverage (60–180 km swaths)	PRO: Orbiting sensors characterized by high spatial resolution (12–20 m) and wide coverage (25–300 km swaths)
	PRO: Most optical systems are multi-spectral, allowing use of multiple bands to discriminate crop and soil conditions	CON: Currently orbiting SAR sensors (i) are not multi-frequency and (ii) are only low-frequency (C- or L-band)

† Speckle is the combination of scattering from lots of small scatterers within a pixel that causes the "grainy" appearance of the radar images. This effect can be alleviated by averaging several radar measurements together (through multi-looking or post-processing) to reduce variation with a consequent reduction in spatial resolution.

Table 2. Characteristics of four orbiting SAR sensors.

	ERS-1, ERS-2	JERS-1	Radarsat
Wavelength	5.7 cm (C)	23.5 cm (L)	5.7 cm (C)
Polarization	VV	HH	HH
Resolution	25 m	25 m	10–30 m
Swath Width	100 km	80 km	50–170 km
Incidence Angle†	23°	38°	17°–43°

† SAR scattering is strongly dependent on incidence angle (θ_i), e.g., specular reflection occurs at θ_i=0° and small changes in surface elevation are more easily visible at near-grazing angles (θ_i~80°-90°). Smooth vs. rough surfaces are easier to detect at θ_i>20°.

BACKGROUND AND THEORY

In the reflective region of the optical spectrum, discrimination of crop growth and plant status is generally accomplished by assessing the reflectance of red and near-infrared (NIR) reflectance (ρ_{Red} and ρ_{NIR}, respectively) of the plant canopy. Simply put, plants absorb red radiation and scatter NIR radiation resulting in a large difference between ρ_{NIR} and ρ_{Red}; in contrast, for bare soil, $\rho_{NIR} \approx \rho_{Red}$. This difference between plant and soil reflectances is often enhanced by computing a ratio of visible and near-infrared reflectances, termed a Vegetation Index (VI). A commonly-used VI is the Soil Adjusted Vegetation Index

$$SAVI = (\rho_{NIR}-\rho_{Red})/(\rho_{NIR}+\rho_{Red}+L)(1+L), \quad [1]$$

where L is a unitless constant assumed to be 0.5 for a wide variety of leaf area index values (Huete, 1988). SAVI has been found to be sensitive to such vegetation parameters as green leaf area index (GLAI), fraction absorbed photosynthetically active radiation, and percentage of the ground surface covered by vegetation.

In the thermal region, remotely sensed measurements of soil and foliage temperature have been linked to soil moisture content, plant water stress, and plant transpiration rate (e.g., Jackson, 1982). The sensitivity of surface temperature to plant and soil moisture conditions is related primarily to the heat loss associated with evaporation and transpiration. As such, the thermal signal is related to the percentage of the site covered by vegetation and the water status of the vegetation and soil (i.e., EvapoTranspiration or ET).

In the microwave region, specifically the C-band SAR wavelength (Table 3), it is generally assumed that σ^o is directly related to surface roughness, soil moisture and vegetation density. This can be expressed by the water-cloud model, in which the power backscattered by the whole canopy σ^o is the sum of the contribution of the vegetation σ^o_v and that of the underlying soil σ^o_s. The latter is attenuated by the vegetation layer as a function of τ^2, the two-way attenuation through the canopy. Thus,

$$\sigma^o = \sigma^o_v + \tau^2\sigma^o_s, \quad [2]$$

where τ^2 is a function of green leaf area index (GLAI), σ^o_v is a function of τ^2 and GLAI, and σ^o_s is a function of volumetric soil moisture content (h_v) and surface roughness (Ulaby et al., 1984; Prevot et al., 1993).

It is apparent from this short discussion that there is a relation between the optical and SAR sensitivities to variations in soil surface roughness, vegetation cover, and soil moisture (Table 4). Theoretically, as the surface roughness increases, σ^o increases due to increased SAR scattering, ρ_{Red} and ρ_{NIR} decrease due to increased surface shadows, and T_s and SAVI remain relatively unchanged. As crop cover decreases, σ^o increases due to an increase in τ^2, T_s increases due to decreased transpiration rate, ρ_{Red} increases due to decreased leaf chlorophyll, ρ_{NIR} decreases due to decreased leaf scattering, and the SAVI decreases dramatically. As surface soil moisture increases, σ^o increases due to a change in the surface dielectric constant, T_s decreases due to increased evaporation rate, ρ_{Red} and ρ_{NIR} decrease due to water absorption, and the SAVI remains relatively unchanged.

Table 3. Specifications and characteristics of commonly-used SAR spectral bands.

Spectral Band	Wave-length	Examples of SAR responses to agricultural targets
X	~3 cm	**Shorter wavelengths** are sensitive to plant parameters such as GLAI, plant biomass, and % vegetation cover; **Longer wavelengths** are sensitive to surface (1–5 cm) soil moisture content and attenuated by increasing vegetation cover; **All wavelengths** are sensitive to variations in surface roughness and topography (Prevot et al., 1993; Ulaby et al., 1994; Moran et al., 1997b, 1998)
C	~6 cm	
L	~24 cm	
P	~70 cm	

Table 4. Theoretical response of Optical and SAR measurements to changes in plant–soil condition.

Change in Plant–Soil Condition	σ^o	T_s	ρ_{Red}	ρ_{NIR}	SAVI
Increase in surface roughness	↑	–	↓	↓	–
Decrease in vegetation biomass	↑	↑	↑	↓	↓
Increase in surface soil moisture content	↑	↓	↓	↓	–

↑ indicates an increase, ↓ indicates a decrease, and – indicates no substantial change. σ^o is backscatter, T_s is surface temperature, ρ_{Red} and ρ_{NIR} are surface reflectance in the Red and NIR spectrum, and SAVI is the soil adjusted vegetation index.

For analysis of the SAR information, we defined a set of normalized difference (Δ_N) indices, where

$$\Delta_N\sigma^o = (\sigma^o_1 - \sigma^o_2)/(\sigma^o_X - \sigma^o_M), \quad [3]$$

$$\Delta_N T_s = (T_{s1} - T_{s2})/(T_{sX} - T_{sM}), \quad [4]$$

$$\Delta_N\rho_{Red} = (\rho_{Red1} - \rho_{Red2})/(\rho_{RedX} - \rho_{RedM}), \quad [5]$$

$$\Delta_N\rho_{NIR} = (\rho_{NIR1} - \rho_{NIR2})/(\rho_{NIRX} - \rho_{NIRM}), \quad [6]$$

$$\Delta_N SAVI = (SAVI_1 - SAVI_2)/(SAVI_X - SAVI_M), \quad [7]$$

and the subscripts 1 and 2 refer to two locations within the field, and subscripts X and M refer to the maximum and minimum values within the entire farm. These indices range from -1 to 1, and are indicative of the optical and SAR responses to changes in plant/soil condition summarized in Table 4.

EXPERIMENT

The site of the Agricultural SAR/Optical Synergy (ASOS) study was the University of Arizona Maricopa Agricultural Center (MAC). MAC is a 770 ha research and demonstration farm located about 48 km south of Phoenix. The demonstration farm is composed of large fields (up to 0.27 * 1.6 km) in which alfalfa is grown year-round, cotton is grown during the summer, and wheat is grown during the winter. A data management system is in place to archive planting, harvesting and tillage information, and the times and amounts of water, herbicide and pesticide applications. Since the predominant irrigation method for the MAC demonstration farm is flooding, each field is dissected into level-basin borders.

The ASOS study was conducted in two parts. A retrospective study was conducted based on existing images in the European Space Agency (ESA) and EROS Data Center (EDC) archives. These images from 1995 and 1996 were ordered with the intent of determining field soil moisture, vegetation cover, and tillage conditions based on the response of the optical and SAR signals, and validating these determinations with the field notes archived by the MAC Farm Manager. A second study was conducted in which we ordered TM/SAR image pairs for three dates (May, June, and July) in 1997. During all three overpasses, we arranged for one field to be flood irrigated such that a large portion of the field was saturated, and, for contrast, a large portion was completely dry. A kenaf crop was planted in May, and by the June overpass dates, the GLAI was 0.3; by the July overpass, the GLAI was 1.5. We also monitored vegetation and soil moisture conditions in two fields of alfalfa at various growth stages with a variety of soil moisture conditions.

During each TM/SAR overpass in 1997, we made ~50 gravimetric measurements of soil moisture content to 5-cm depth in the dry and wet portions of the fallow field and in the two alfalfa fields. These were converted to volumetric soil moisture using estimates of field bulk density. We also measured GLAI in situ at multiple locations using a LICOR LAI2000 plant canopy analyzer.

The SAR raw data were averaged to one value for each field border (a minimum of 100 pixels) to minimize the speckle effect, and the mean was converted to values of σ^o according to Moran et al. (1997b). The TM raw data were converted to values of apparent reflectance and radiometric temperature according to Moran et al. (1995) and Markham and Barker (1986). The term apparent reflectance refers to reflectance factors derived from satellite images that have not been corrected for atmospheric effects. Considering that the TM data were acquired on days with clear, dry atmospheric conditions, the difference between apparent and surface reflectance in the Red and NIR wavelengths should be minimal. The radiometric temperature (T_r) was converted to surface kinetic temperature (T_s) based on measurements of surface emissivity (ε) using the relation $T_s = (T_r^4/\varepsilon)^{1/4}$, where $\varepsilon = 0.98$ for dense alfalfa, $\varepsilon = 0.95$ for rough bare soil and recently-harvested alfalfa, and $\varepsilon = 0.89$ for laser-leveled bare soil (Reginato & Jackson, 1988).

For a number of reasons, the ASOS study did not go as smoothly as planned. First, there were few TM/SAR pairs available in the ESA and EDC archives. We were only able to obtain images for November and December 1995 and 1996 (Table 5). During this time of year, there was very little farm activity, and the only crops were alfalfa and emergent wheat. Second, though we ordered the ERS-2 SAR and Landsat TM images for May, June, and July 1997, we only received one SAR/TM image pair (May 1997; Fig. 1). The reason for the failure to obtain the images as ordered is still unknown; however, such acquisition failure is not uncommon for satellite-based sensors, as reported by Moran (1994).

Table 5. ERS-2 SAR and Landsat TM scenes ordered for the 1995–1996 Agricultural SAR/Optical Synergy (ASOS) Study.

ERS-2 SAR	Landsat-5 TM	Notes
6 Nov. 1995	8 Nov. 1995	Wheat planted; cotton harvested; several disked fields; no irrigations
11 Dec. 1995	10 Dec. 1995	
25 Nov. 1996	26 Nov. 1996	
30 Dec. 1996	28 Dec. 1996	
19 May 1997	21 May 1997	Soil moisture study with bare soil conditions in Field 3
23 June 1997	22 June 1997	Soil moisture study with kenaf GLAI = 0.3 in Field 3 *SAR scene not acquired by ESA*
10 July 1997	9 July 1997	Soil moisture study with kenaf GLAI = 1.5 in Field 3 *Neither the SAR nor TM scene was acquired*

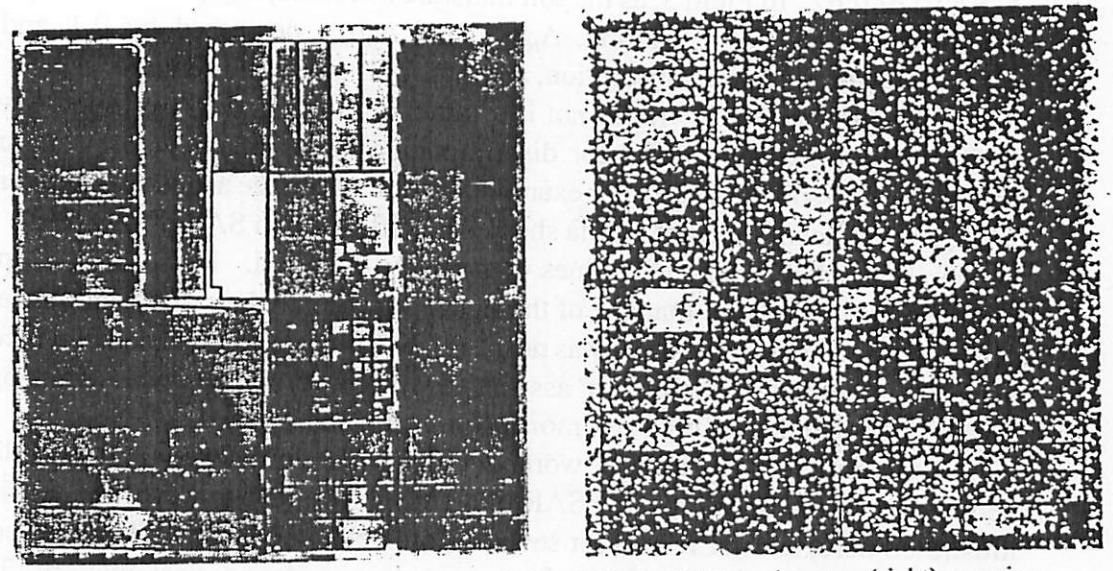

Fig. 1. Images of Landsat TM reflectance (left) and ERS-2 SAR backscatter (right) covering Maricopa Agricultural Center acquired on 21 May and 19 May 1997, respectively. The vector overlay designates the MAC field borders, and the total area covers 770 hectares.

RESULTS AND DISCUSSION

Retrospective ASOS Study 1995–1996

For this preliminary analysis, we selected all MAC fields in the four 1995–1996 images that had a record of distinctive within-field differences in tillage, soil moisture, and vegetation density. Since results were similar for fields of similar surface conditions, three fields were selected as examples for illustration in this section. According to field notes and on-site observations, Field 1 was fallow, but part of the field had been laser leveled and part was still rough due to cultivation; Field 2 was planted with alfalfa, but one-half of the field had been recently harvested, and Field 3 was also fallow, but part of the field had been flood irrigated.

All three fields (numbered 1 to 3 for reference herein) had a notable increase in the SAR σ^o ($\Delta_N\sigma^o$ ~ 0.2) from one end of the field to the other (Fig. 2 and 3). The increase in $\Delta_N\sigma^o$ in Field 1 was due to the increased scattering of the SAR signal due to soil roughness. In Field 2, the increase in $\Delta_N\sigma^o$ resulted from a decrease in the alfalfa crop density due to a recent harvest, resulting in a larger τ^2 value in Eq. [2]. In Field 3, $\Delta_N\sigma^o$ increased due to the change in soil moisture and the sensitivity of the SAR signal to the dielectric constant of the surface. The dielectric constant of water is about 80 (in the C-band wavelength) and that of dry vegetation or soil is about 2 to 3.

The visual and quantitative assessment presented in Fig. 2 and 3 showed that the response of the optical data to the three different field conditions corresponded well with the theoretical hypotheses presented in Table 4. In Field 1, as the soil roughness increased, $\Delta_N\rho_{NIR}$ and $\Delta_N\rho_{Red}$ decreased by 0.2 due to increased surface shadows, and $\Delta_N T_s$ and Δ_NSAVI remained near zero for the two roughnesses. In Field 2, as the vegetation decreased due to harvest, $\Delta_N T_s$ increased by about 0.2 due to the decrease in transpiration, $\Delta_N\rho_{NIR}$ decreased by 0.5 and $\Delta_N\rho_{Red}$ increased by 0.4 due to the decrease in leaf area and photosynthetic activity, causing a decrease in Δ_NSAVI of 0.62. In Field 3, as the soil moisture increased, $\Delta_N T_s$ decreased by about 0.5 due to evaporative cooling, $\Delta_N\rho_{NIR}$ and $\Delta_N\rho_{Red}$ decreased by 0.1 and 0.2 respectively due to water absorption, and Δ_NSAVI remained near zero.

Based on data for fields not illustrated in Fig. 2 and 3, we found that the optical data were also useful for discriminating mixes of effects of roughness, vegetation and soil moisture. For example, in the SAR image acquired in November 1995, two adjacent fields of alfalfa showed no difference in SAR σ^o ($\Delta_N\sigma^o$~0). Yet, we computed large negative values of $\Delta_N T_s$ and Δ_NSAVI. Based on the optical response, we postulated that one of the fields was recently harvested and had a low soil moisture content; the other was near full vegetation cover and had been recently irrigated. As a result, the high σ^o associated with low crop cover was offset by the low σ^o associated with high soil moisture content, and $\Delta_N\sigma^o$~0.

Overall, the Δ_N indices worked well to discriminate the causal relation between surface conditions and SAR σ^o. Though results for only three fields are illustrated here, similar results for several more fields showed that this method has potential for interpretation of SAR imagery with coincident optical imagery. These results also illustrated the sensitivity of Landsat TM and ERS-2 SAR imagery to differences in tillage, surface soil moisture, and vegetation density.

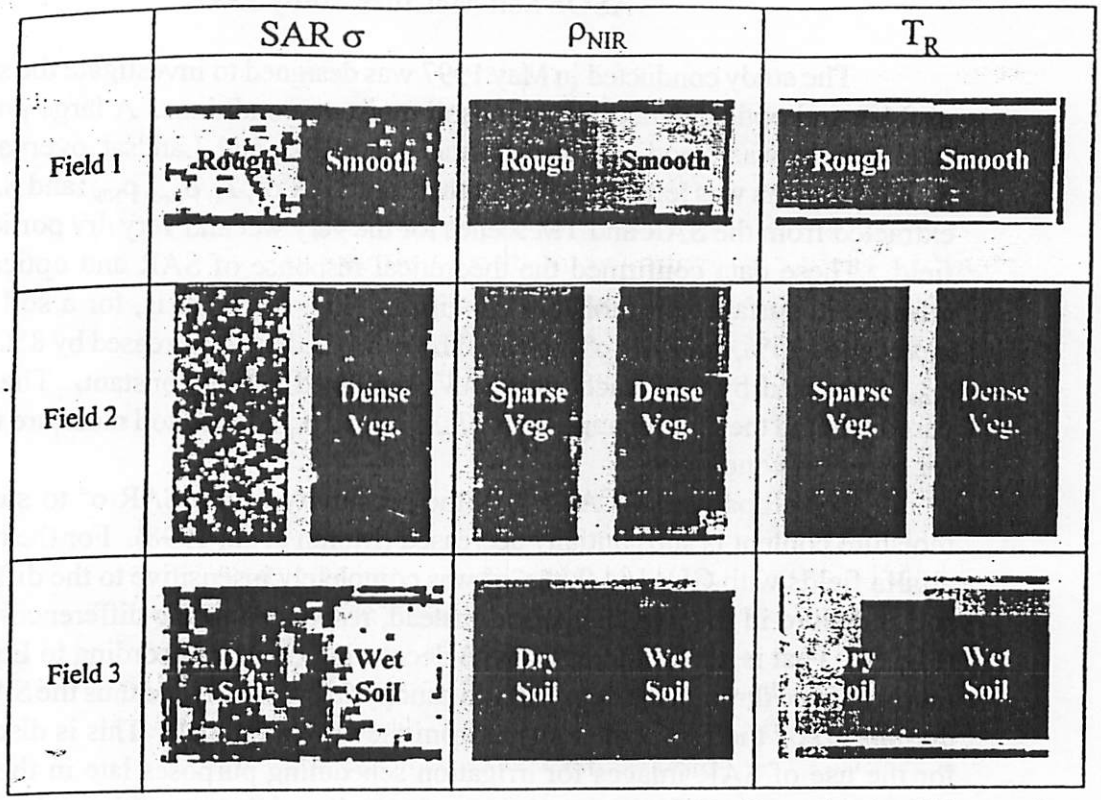

Fig. 2. Extracts of SAR and optical data for the three study fields, illustrating the differences in spectral response in SAR backscatter (σ), NIR reflectance (ρ_{NIR}), and radiometric surface temperature (T_r) to variations in field tillage, vegetation density, and surface soil moisture.

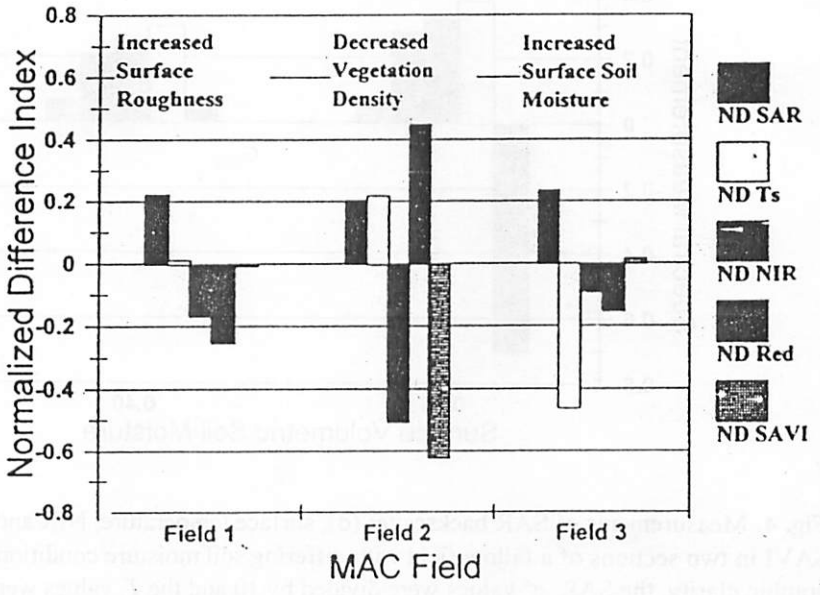

Fig. 3. The response of Δ_N indices (Eq. [3]-[7]) to variations in field roughness, vegetation density and surface soil moisture. The five legend captions refer to $\Delta_N\sigma^o$, $\Delta_N T_s$, $\Delta_N\rho_{Red}$, $\Delta_N\rho_{NIR}$, and Δ_NSAVI, respectively.

ASOS Soil Moisture Study 1997

The study conducted in May 1997 was designed to investigate the sensitivity of SAR and optical data to differing soil moisture conditions. A large portion of a fallow field was flood irrigated during the ERS-2 and Landsat overpasses, and another portion was left dry. Measurements of SAR σ^o, T_s, ρ_{Red}, ρ_{NIR}, and SAVI were extracted from the SAR and TM scenes for the very wet and very dry portions of the field. These data confirmed the theoretical response of SAR and optical data to changes in surface soil moisture conditions (Fig. 4). That is, for a soil moisture increase of 35%, the SAR σ^o increased by nearly 8 dB, T_s decreased by 8°C, ρ_{Red} and ρ_{NIR} decreased by 0.07 each, and SAVI remained nearly constant. These results demonstrated the large changes in σ^o, T_s, ρ_{Red}, and ρ_{NIR} due to soil moisture variations for bare soil conditions.

For crops with GLAI > 1.0, the sensitivity of the SAR σ^o to surface soil moisture content is substantially decreased (Moran et al., 1998). For the two MAC alfalfa fields with GLAI~4.0, the σ^o was completely insensitive to the difference in soil moisture in the two fields, and instead, responded to the differences in GLAI (Fig. 5). That is, the σ^o increased with decreasing GLAI. According to Eq. [2], the transmittance through the dense alfalfa canopy (τ^2) was low, and thus the SAR σ^o was dominated by the backscatter signal from the vegetation (σ^o_v). This is discouraging for the use of SAR images for irrigation scheduling purposes late in the growing season. However, information about surface soil moisture conditions obtained early in the growing season will still be useful for monitoring irrigation efficacy, mapping precipitation events, and determining soil texture.

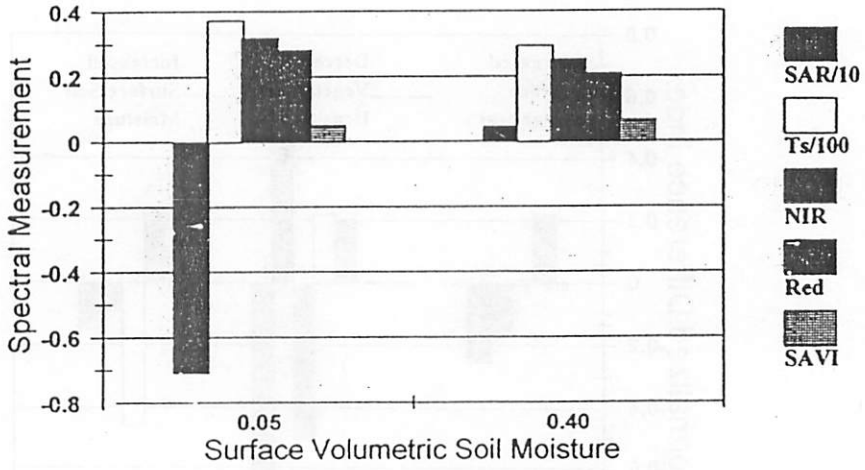

Fig. 4. Measurements of SAR backscatter (σ), surface temperature, NIR and Red reflectance and SAVI in two sections of a fallow field with differing soil moisture conditions. For purposes of graphic clarity, the SAR σ^o values were divided by 10 and the T_s values were divided by 100.

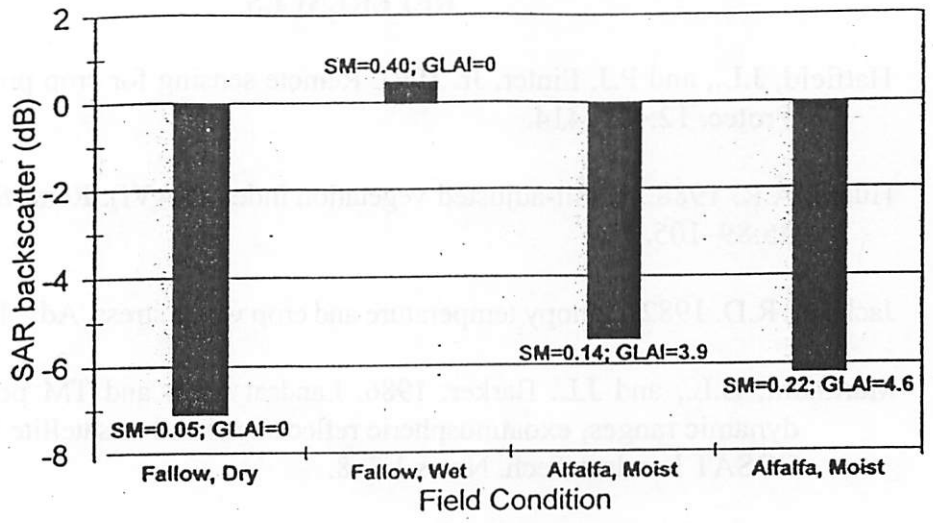

Fig. 5. A comparison of the sensitivity of SAR backscatter to soil moisture and vegetation density conditions for a fallow field and an alfalfa field. In the figure, the bars are labeled with measurements of volumetric soil moisture (SM) and green leaf area index (GLAI).

CONCLUDING REMARKS

The objective of this study was to investigate the utility of SAR images for precision farm management applications. These preliminary results showed that the SAR σ° was sensitive to differences in field roughness (related to tillage), vegetation density, and surface soil moisture. Furthermore, we found that optical imagery obtained coincident with SAR imagery allowed a better understanding of the interactions of the SAR signal with soil and plant surfaces. Thus, it may be possible to model SAR σ° based on optical measurements rather than the time-consuming *in situ* measurements of surface roughness and GLAI. Future work on this data set will be focused on compiling the SAR, optical and field information necessary to develop a relation to facilitate interpretation of the SAR image, which may take the form

$$\Delta_N\sigma = a + b\Delta_N T_s + c\Delta_N\rho_{NIR} + d\Delta_N\rho_{Red} + e\Delta_N SAVI, \quad [8]$$

where the parameters *a-e* are empirical coefficients determined by multiple regression analysis. Recognizing the limitations of optical remote sensing data due to cloud interference and atmospheric attenuation, the findings of this study should encourage further studies of SAR imagery for crop and soil assessment.

ACKNOWLEDGMENTS

We would like to acknowledge valuable help from Wanmei Ni, Chandra Holifield, Ross Bryant, Robin Marsett, and Michael Helfert, and the cooperation of personnel at the Univ. of Arizona Maricopa Agricultural Center (MAC). Financial support was provided by the NASA Landsat Science Team (NASA S-41396-F), NASA EOS IDS (NAGW-2425), and European Space Agency (ESA-AO2.F119).

REFERENCES

Hatfield, J.L., and P.J. Pinter, Jr. 1993. Remote sensing for crop protection. Crop Protec. 12:403–414.

Huete, A.R. 1988. A soil-adjusted vegetation index (SAVI). Rem. Sens. Environ. 25:89–105.

Jackson, R.D. 1982. Canopy temperature and crop water stress. Adv. Irrig. 1:43–85.

Markham, B.L., and J.L. Barker. 1986. Landsat MSS and TM post-calibration dynamic ranges, exoatmospheric reflectances and at-satellite temperatures. EOSAT Landsat Tech. Notes 1:3–8.

Moran, M.S. 1994. Irrigation management in Arizona using satellites and airplanes. Irrig. Sci. 15:35–44.

Moran, M.S., R.D. Jackson, T.R. Clarke, J. Qi, F. Cabot, K.J. Thome, and B.L. Markham. 1995. Reflectance factor retrieval from Landsat TM and SPOT HRV data for bright and dark targets. Rem. Sens. Environ. 52:218–230.

Moran, M.S., Y. Inoue, and E.M. Barnes. 1997a. Opportunities and limitations for image-based remote sensing in precision crop management. Rem. Sens. Environ. 61:319–346.

Moran, M.S., A. Vidal, D. Troufleau, J. Qi, T.R. Clarke, P.J. Pinter, Jr., T.A. Mitchell, Y. Inoue, and C.M.U. Neale. 1997b. Combining multi-frequency microwave and optical data for farm management. Rem. Sens. Environ. 61:96–109.

Moran, M.S., A. Vidal, D. Troufleau, Y. Inoue, and T.A. Mitchell. 1998. Ku- and C-band SAR for discriminating agricultural crop and soil conditions. IEEE Geosci. Rem. Sens. 36:265–272.

Prevot, L., I. Champion and G. Guyot. 1993. Estimating surface soil moisture and leaf area index of a wheat canopy using dual-frequency (C and X bands) scatterometer. Rem. Sens. Environ. 46:331–339.

Reginato, R.J., and R.D. Jackson. 1988. Emissivity measurements of soil and plant surfaces. p. 9. *In* The MAC III Experiment Report. USDA-ARS U.S. Water Conserv. Lab., Phoenix, AZ.

Ulaby, F.T., C.T. Allen, G. Eger III, and E. Kanemasu. 1984. Relating the microwave backscattering coefficient to leaf area index. Rem. Sens. Environ. 14:113–133.